Virologica Sinica (2018) 33:515–523
https://doi.org/10.1007/s12250-018-0067-5

www.virosin.org
www.springer.com/12250

RESEARCH ARTICLE

Japanese Encephalitis Virus NS1′ Protein Antagonizes Interferon Beta Production

Dengyuan Zhou[1,2,3] · Fan Jia[4] · Qiuyan Li[1,2,3] · Luping Zhang[1,2,3] · Zheng Chen[1,2,3] · Zikai Zhao[1,2,3] · Min Cui[1,2,3] · Yunfeng Song[1,2,3] · Huanchun Chen[1,2,3] · Shengbo Cao[1,2,3] · Jing Ye[1,2,3]

Received: 27 September 2018 / Accepted: 7 November 2018 / Published online: 12 December 2018

Abstract

Japanese encephalitis virus (JEV) is a mosquito-borne virus and the major cause of viral encephalitis in Asia. NS1′, a 52-amino acid C-terminal extension of NS1, is generated with a -1 programmed ribosomal frameshift and is only present in members of the Japanese encephalitis serogroup of flaviviruses. Previous studies demonstrated that NS1′ plays a vital role in virulence, but the mechanism is unclear. In this study, an NS1′ defected (rG66A) virus was generated. We found that rG66A virus was less virulent than its parent virus (pSA14) in wild-type mice. However, similar mortality caused by the two viruses was observed in an IFNAR knockout mouse model. Moreover, we found that rG66A virus induced a greater type I interferon (IFN) response than that by pSA14, and JEV NS1′ significantly inhibited the production of IFN-β and IFN-stimulated genes. Taken together, our results reveal that NS1′ plays a vital role in blocking type I IFN production to help JEV evade antiviral immunity and benefit viral replication.

Keywords Japanese encephalitis virus (JEV) · NS1′ · Type I interferon (IFN-I) · Immune evasion

Introduction

Japanese encephalitis virus (JEV) is a member of the genus *Flavivirus* within the family *Flaviviridae*. It is one of the most important mosquito-borne viruses and causes serious viral-encephalitis in East and Southeast Asia (Mackenzie *et al.* 2004; Sucharit *et al.* 1989; van den Hurk *et al.* 2009). Recently, this virus has spread to other geographic areas such as Australia, Pakistan, and Saipan following global warming and urbanization (Igarashi *et al.* 1994; Johansen *et al.* 2001; Mackenzie 2005; Mitchell *et al.* 1993). Japanese encephalitis (JE) has a mortality of 10%–50%, and approximately half of JE survivors have severe neurological sequelae (Turtle and Solomon 2018). Although vaccines against JEV have been used for many years, more than 50,000 meningoencephalitis cases and approximately 15,000 deaths are reported each year (Ginsburg *et al.* 2017; Turtle and Driver 2018).

The JEV genome is a single-stranded positive-sense RNA of approximately 11 kb. It encodes a single large polyprotein, which is cleaved by viral and host proteases to produce three structural proteins (capsid, premembrane, and envelope) and seven nonstructural (NS) proteins (NS1, NS2A/B, NS3, NS4A/B, and NS5) (Morita *et al.* 2015; Unni *et al.* 2011). NS1 protein is a nonstructural protein involved in many crucial biological events during viral infection and spreading, such as viral replication and virulence, immune invasion, and activation of the host complementary system (Amorim *et al.* 2014; Muller and Young 2013; Rastogi *et al.* 2016). NS1′, a 52 amino acid C-terminal extension of NS1, was first detected in JEV-infected cells generated by a -1 programmed ribosomal frameshift

Electronic supplementary material The online version of this article (https://doi.org/10.1007/s12250-018-0067-5) contains supplementary material, which is available to authorized users.

✉ Jing Ye
yej@mail.hzau.edu.cn

1 State Key Laboratory of Agricultural Microbiology, Huazhong Agricultural University, Wuhan 430070, China

2 Key Laboratory of Preventive Veterinary Medicine in Hubei Province, College of Veterinary Medicine, Huazhong Agricultural University, Wuhan 430070, China

3 The Cooperative Innovation Center for Sustainable Pig Production, Huazhong Agricultural University, Wuhan 430070, China

4 Wuhan Institute of Physics and Mathematics (WIPM), Chinese Academy of Sciences, Wuhan 430070, China

(PRF) via a slippery heptanucleotide (YCCUUUU) and potential pseudoknot nearby (Blitvich *et al.* 1999; Firth and Atkins 2009). It has been reported that NS1′ in West Nile virus (WNV) and JEV play important roles in neuroinvasiveness, but the mechanism has not been clarified (Melian *et al.* 2010; Wang *et al.* 2015; Ye *et al.* 2012).

As one of the most crucial host defense molecules, type I interferon (IFN-I) is essential for combating viral infections. To improve better survival, viruses develop different strategies to antagonize IFN-I (Snell and Brooks 2015; Teijaro 2016). Efficient replication of flaviviruses is closely linked with their ability to inhibit IFN-I production and signaling pathways (Best 2017; Urosevic 2003). For example, WNV NS1 inhibits IFN-I production by targeting RIG-I and MDA5 (Zhang *et al.* 2017); Dengue (DENV) and Zika virus NS5 antagonizes IFN-I signaling by degrading STAT2 (Ashour *et al.* 2009; Grant *et al.* 2016). However, few functions have been reported for flavivirus NS1′ in inhibiting IFN-I production and signaling pathways.

In this study, a defective NS1′ virus was generated to investigate the mechanism of how NS1′ protein contributes to JEV pathogenesis. We found that the lower virulence of defective NS1′ virus is related to IFN-I signaling in the host. Mechanistically, we demonstrated that NS1′ protein antagonizes the production of IFN-β and IFN-stimulated genes (ISGs), promoting the replication of JEV.

Materials and Methods

Cells and Viruses

Baby hamster kidney (BHK-21) cells, mouse testicular Sertoli (TM4) cells, African green monkey kidney (Vero) cells, human cervix epithelial (HeLa) cells, and human lung epithelial (A549) cells were stored in the laboratory and cultured in Dulbecco's Modified Eagle's Medium (DMEM; Sigma, St. Louis, MO, USA) supplemented with 10% fetal bovine serum (GIBCO, Grand Island, NY, USA), 100 U/mL penicillin, and 100 mg/mL streptomycin (Sigma) at 37 °C and 5% CO_2.

The parental JEV (pSA14) and NS1′ defective viruses (rG66A, a 'G'-to-'A' mutation at nucleotide position 66 in the NS2A gene of SA14 of JEV) were produced by electroporation of BHK-21 cells with transcribed RNA from the full-length cDNA clones pMW218-JEV-rAT and pMW218-JEV-NS2A-G66A, respectively, which were kindly provided by Fan Jia (Wuhan Institute of Physics and Mathematics, Chinese Academy of Sciences).

Plasmid Construction

The plasmids pcDNA3.1-NS1 and pcDNA3.1-NS1′ encoding the JEV NS1 protein and NS1′ protein were constructed by polymerase chain reaction (PCR) using JEV-SA14 cDNA as a template and then cloned into the pcDNA3.1(+) vector. The primers were listed in Supplementary Table S1.

Protein and Antibodies

Mouse monoclonal antibody against JEV NS1 (2B8) and NS1′ was generated in our laboratory. Briefly, mice were immunized with purified JEV NS1 protein and the monoclonal antibodies were produced and isolated by using hybridoma technology. Clone 2B8 which shows the highest specificity and sensitivity against JEV NS1 was used in this study. Commercial antibodies, including anti-GAPDH antibodies (ABclonal Technology, Woburn, MA USA), horseradish peroxidase-conjugated goat anti-mouse IgG (Boster, Wuhan, China), and Alexa Fluor 488-conjugated goat anti-mouse IgG (Invitrogen, Carlsbad, CA, USA) were used.

Western Blotting

Cell lysates were generated in cell lysis buffer (Beyotime Biotechnology, Shanghai, China) for 20 min at 4 °C. The protein concentration was determined by using a BCA protein assay kit (Thermo Scientific, Waltham, MA, USA) and boiled at 95 °C for 15 min. Equivalent amounts of proteins were separated by sodium dodecyl sulfate polyacrylamide gel electrophoresis (12% polyacrylamide) and electroblotted onto a polyvinylidene fluoride membrane (Millipore, Billerica, MA, USA) using a Mini Trans-Blot Cell (Bio-Rad, Hercules, CA, USA). The membrane was incubated with the relevant antibodies for 2 h at room temperature (RT, approximately 20–30 °C) or overnight at 4 °C. After washing three or four times with TBST (50 mmol/L Tris–HCl, 150 mmol/L NaCl, and 0.1% Tween 20, pH 7.4), the membrane was incubated with horseradish peroxidase-labeled goat anti-mouse IgG at RT for 30–45 min, and then visualized with a chemiluminescence system (Bio-Rad).

Transfection

HeLa cells in 12-well plates (at a density of 2×10^5/well) were transfected with the relevant expression plasmids (pcDNA3.1-NS1 or pcDNA3.1-NS1′) or an empty control plasmid (pcDNA3.1) (800 ng) using Lipofectamine 2000 (Invitrogen) for 24 h and then transfected with 5 μg poly(I:C) for another 12 h. For viral infection experiments, HeLa cells were transfected with plasmids for 12 h and then infected with JEV-pSA14 or rG66A for another 24 h.

Quantitative RT-PCR

Total RNA of cells was extracted according to the instructions of TRIzol Reagent (Invitrogen). The concentration of RNA was measured, and cDNA was synthesized by reverse transcription using a ReverTra Ace RT kit (Toyobo, Osaka, Japan). Real-time PCR was performed according to the instructions of the SYBR green real-time PCR master mix (Toyobo) and fluorescence intensity was analyzed with an ABI StepOne Plus system (Applied Biosystems, Foster City, CA, USA). The results were normalized to β-actin expression in each sample. The primers were listed in supplementary Table S1.

Plaque Assay

A549 or TM4 cells were infected with pSA14 and rG66A virus at a multiplicity of infection (MOI) of 1.0. At 12, 24, 36, and 48 h post-infection, the supernatant was harvested and stored at −80 °C. The samples were used to infect BHK-21 cells by serially 10-fold dilution in 12-well plates. After incubation for 1.5 h, the cells were washed with PBS and cultured in DMEM containing 2% fetal bovine serum and 1.5% sodium carboxymethyl cellulose (Sigma) for 4 or 5 days. Next, visible plaques were counted, and viral titers were calculated.

Inoculation of Mice with JEV

Adult C57BL/6 J mice (female, 5-weeks-old, HZAUMO-2017-016) were obtained from Scientific Ethic Committee of Huazhong Agriculture University (Wuhan, China), while IFNAR knockout ($IFNAR^{-/-}$) C57BL/6 J mice were kindly provided by Bin Wei (Wuhan Institute of Virology, Chinese Academy of Sciences). The mice were maintained according to Committee for Protection, Supervision, and Control of Experiments on Animals guidelines, Huazhong Agricultural University.

Five-week-old C57BL/6 J mice were injected intracranially with 20 μL containing 200 PFU of pSA14 and rG66A virus diluted with DMEM. Control animals were injected with 20 μL serum-free DMEM by the same route. The day of injection was referred to as day 0. Five-week-old C57BL/6 J or $IFNAR^{-/-}$ mice were injected intraperitoneally with 200 μL containing 1×10^6 PFU of pSA14 and rG66A virus diluted with DMEM. Control animals were injected with 200 μL DMEM by the same route.

The presentation of clinical signs of disease and mortality in mice were monitored every day. Clinical signs of disease were divided into seven grades, including subclinical, ruffled fur and hunched, hindlimb weakness, mild paresis, moderate paresis, severe paresis, and moribund or dead (Daniels *et al.* 2017).

Quantification and Statistical Analysis

Statistical analyses of all data were conducted by using Prism (6.0) (GraphPad, Inc., San Diego, CA, USA). The log-rank test was used to analyze survival experiments. The differences in all other experiments were analyzed by Student's t test or two-way analysis of variance. A P value < 0.05 was considered as significant for all comparisons.

Results

G66A Mutation in JEV NS2A Abolishes NS1′ Protein Production

Nucleotide 66 of the *NS2A* gene is critical for producing the NS1′ protein. The G 66 in the NS2A coding region was mutated into an A in pMW218-JEV-rAT, which is the full-length cDNA clone of the JEV SA14 strain (Fig. 1A). This silent point mutation did not alter the amino acid sequence of NS2A protein. To clarify whether NS1′ protein function was abolished, we infected BHK-21 cells with wild-type virus (pSA14) and NS1′ defective virus (rG66A) at an MOI of 1, and cell lysates were harvested at 48 h post-infection. As expected, both NS1 and NS1′ protein were detected in pSA14-infected BHK-21 cells, while only NS1 protein was detected in rG66A-infected BHK-21 cells (Fig. 1B).

NS2A G66A Mutation Reduces Virulence of JEV in Mice Relying on IFN-I Response

To determine the role of NS1′ in JEV infection, we compared the neuro-virulence and peripheral-virulence of rG66A and WT virus in C57BL/6 J mice (5-week-old) by intracerebral (i.c.) or intraperitoneal (i.p.) injection. All mice injected intracerebrally with 200 PFU of pSA14 or rG66A virus died within 9 days (Fig. 2A). The survival and clinical signs of disease in mice infected with rG66A

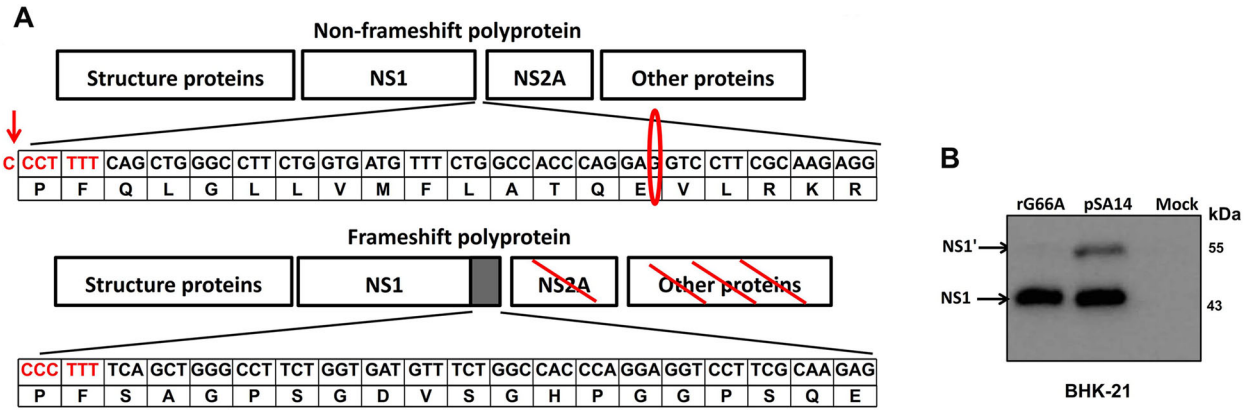

Fig. 1 Recovery and characterization of the rG66A mutant virus. (**A**) Schematic depiction of the translational pathway of non-PRF and PRF flavivirus polyprotein. The sequence of flammulated letters indicates the slippery hepta-nucleotide frameshift motif and in flammulated oval is the silent nucleotide mutation (G → A) in pSA14 virus contributing downstream pseudoknot interactions. Flammulated arrow indicates where a -1 programmed ribosomal frameshift in pSA14 virus occurs. The frameshift polyprotein was aborted by a termination codon at 52 amino acids after C-terminal extension of NS1. Numbers in the frame represent nucleotides and amino acids in NS2A gene of JEV SA14. (**B**) BHK-21 cells were infected or mock-infected with pSA14 or rG66A viruses. NS1 and NS1′ proteins were detected by western blotting with anti-NS1 monoclonal antibody (2B8) at 48 h post-infection.

virus were indistinguishable from those of wide type-infected controls. However, compared to pSA14 virus, both morbidity and mortality showed a slight delay in rG66A-infected mice (Fig. 2A, 2B).

Following i.p. injection, all mice infected with pSA14 virus died within 9 days after infection, while only 30% mortality were observed in mice infected with rG66A at day 9 post-infection (Fig. 2C). Higher mortality in pSA14-infected mice was accompanied by earlier and more severe development of clinical signs of disease (Fig. 2D). The typical neurological symptoms of rG66A-infected mice were significantly alleviated. Moreover, lower viral titers were detected in mouse the blood, spleen, and brain in rG66A group at 5 days post-infection (Fig. 2E). Taken together, these data indicate that NS1′ protein plays an important role in viral multiplication in the peripheral tissue.

To clarify whether the different virulence levels of the two viruses in C57BL/6 J mice are linked to the IFN-I response, an IFNAR$^{-/-}$ mouse model (5-week-old) was used. As shown in Fig. 2F and 2G, all mice infected with pSA14 or rG66A virus died within 6 days after infection, and the clinical signs caused by rG66A virus were consistent with those caused by its parental virus. Similar viral loads were observed in the IFNAR$^{-/-}$ mouse blood, spleen, and brain at 5 days post-infection (Fig. 2H). These data collectively suggest that the difference between rG66A and pSA14 virus is linked to the inhibitory effect of NS1′ on the IFN-I response.

NS2A G66A Mutation Enhances IFN-β Expression in JEV-Infected Cells

Next, viral propagation of rG66A and pSA14 was measured in TM4 and A549 cells, which are susceptible to JEV. We found that growth of the rG66A mutant was somewhat reduced compared to pSA14 virus (Fig. 3A, 3B). However, after treatment with an anti-IFNAR polyclonal antibody in the culture media of TM4 and A549 cells for 2 h before infection, the growth difference between the two viruses disappeared (Fig. 3C, 3D). To confirm this result, the growth properties of JEV rG66A and pSA14 were determined in Vero cells, which are IFN-

Fig. 2 Comparison of neurovirulence of pSA14 and rG66A virus in mice. **A**, **B** Groups of 5-week-old C57BL/6 J mice (n = 10 per group) were infected with 2×10^2 PFU through the intracranial route. **C**, **D** Groups of 5-week-old C57BL/6 J mice (n = 10 per group) were infected with 1×10^6 PFU through the intraperitoneal route. **E**, **G** Groups of 5-week-old IFNAR$^{-/-}$ C57BL/6 J mice (n = 8 per group) were infected with 1×10^6 PFU through the intraperitoneal route. Survival curves are presented (**A, C,** and **E**). Presentation of clinical signs of disease on indicated days are presented (**B, D,** and **G**). Five-week-old C57BL/6 J (**F**) mice or IFNAR$^{-/-}$ C57BL/6 J (**H**) mice were infected intraperitoneally with 1×10^6 PFU of WT-pSA14 and rG66A mutant virus. At day 5 following infection, the blood, spleen, and brain were harvested, weighed, homogenized, and assayed for JEV titers via plaque assay. $^*P < 0.05$; $^{**}P < 0.01$; $^{***}P < 0.001$. Error bars represent SEM. ns, no significance. All data are pooled from two independent experiments.

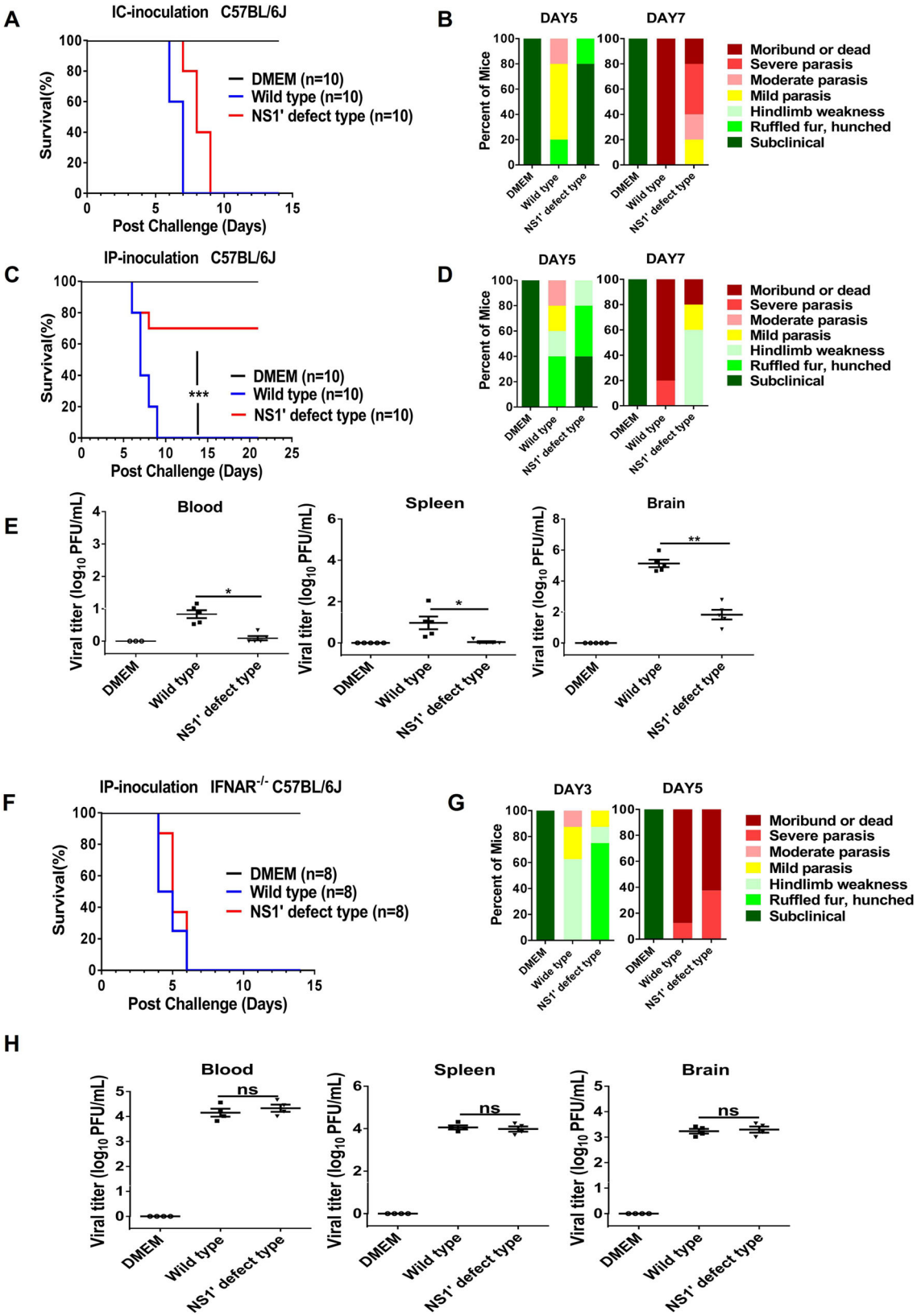
A
IC-inoculation C57BL/6J
Survival(%)
Post Challenge (Days)
DMEM (n=10)
Wild type (n=10)
NS1' defect type (n=10)
B
DAY5
DAY7
Percent of Mice
DMEM
Wild type
NS1' defect type
Moribund or dead
Severe parasis
Moderate parasis
Mild parasis
Hindlimb weakness
Ruffled fur, hunched
Subclinical
C
IP-inoculation C57BL/6J
***
D
E
Blood
Spleen
Brain
Viral titer (log10 PFU/mL)
*
**
F
IP-inoculation IFNAR-/- C57BL/6J
DMEM (n=8)
Wild type (n=8)
NS1' defect type (n=8)
G
DAY3
DAY5
Wide type
H
ns

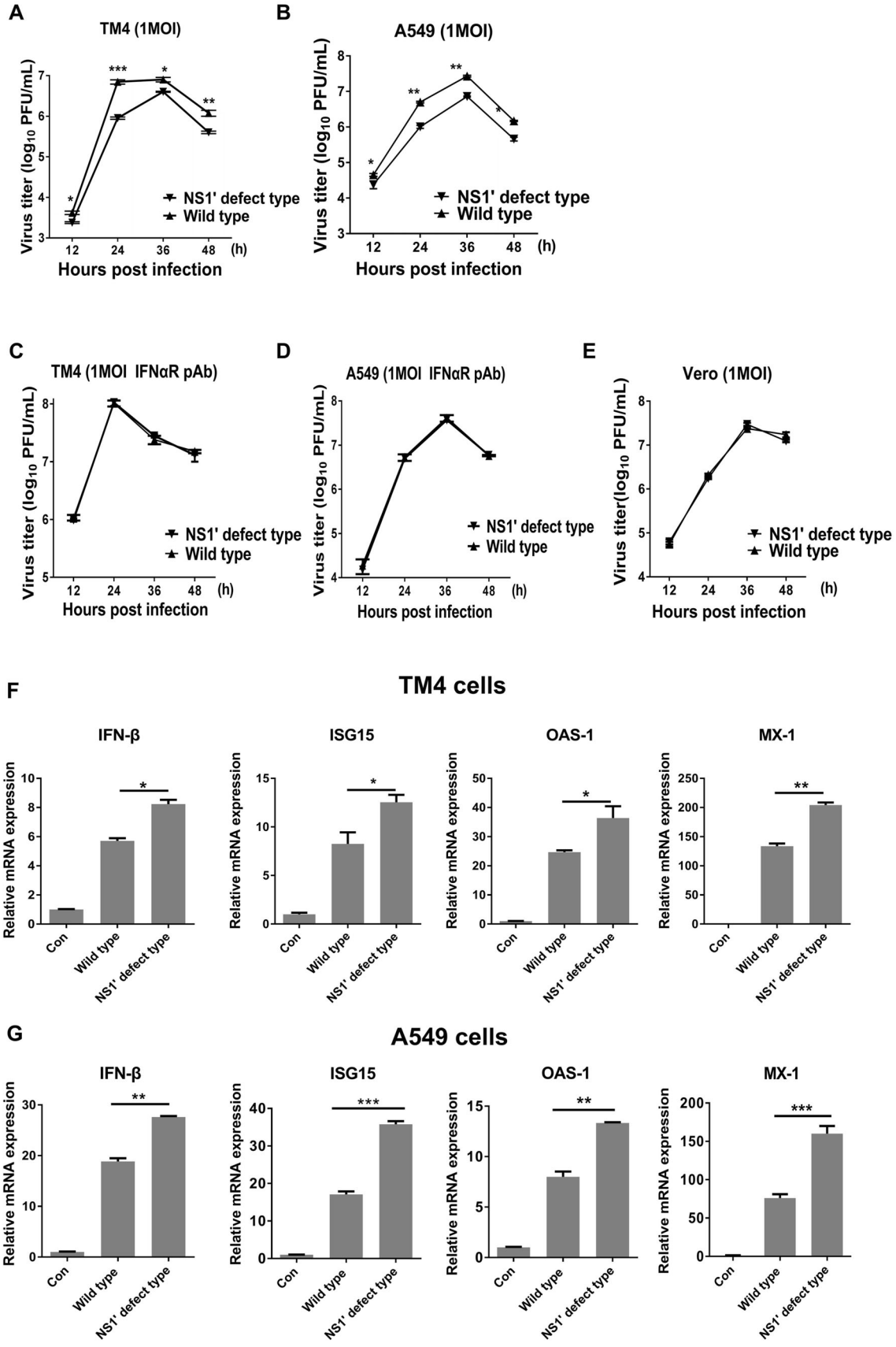
A
TM4 (1MOI)
Virus titer (log10 PFU/mL)
Hours post infection
NS1' defect type
Wild type
B
A549 (1MOI)
C
TM4 (1MOI IFNαR pAb)
D
A549 (1MOI IFNαR pAb)
E
Vero (1MOI)
Virus titer(log10 PFU/mL)
F
TM4 cells
IFN-β
ISG15
OAS-1
MX-1
Relative mRNA expression
Con
Wild type
NS1' defect type
G
A549 cells

◀**Fig. 3** NS2A G66A mutation enhances induction of IFN-β and ISGs expression in cells. **A**, **B** Kinetics of replication of WT-pSA14 or rG66A mutant virus in TM4 (**A**) or A549 (**B**) cells. Cells were infected at an MOI of 1, and the viral titer was measured at 12, 24, 36, and 48 h post-infection using plaque assay of harvested cell supernatant. Growth kinetics from a typical experiment are shown. **C**, **D** Replication kinetics of WT-pSA14 or rG66A mutant virus in TM4 (**C**) or A549 (**D**) cells treated with IFNAR pAb. TM4 and A549 cells were treated with pAb followed by infection of pSA14 or rG66A at an MOI of 1. Viral titer was measured at 12, 24, 36, and 48 h post-infection using plaque assay with harvested cell supernatant. Growth kinetics from a typical experiment are shown. (**E**) Replication kinetics of WT-pSA14 and rG66A mutant virus in Vero cells. Cells were infected with pSA14 or rG66A at an MOI of 1, and the viral titer was measured at 12, 24, 36, and 48 h post-infection using plaque assay with harvested culture fluids. Growth kinetics from a typical experiment is shown. **F**, **G** TM4 (**F**) and A549 (**G**) cells were infected with WT-pSA14 or rG66A mutant virus (MOI = 1). mRNA levels of IFN-β, ISG15, OAS-1, and Mx-1 were determined by qRT-PCR at 24 h post-infection. $*P < 0.05$, $**P < 0.01$, $***P < 0.001$. All data are pooled from two or three independent experiments.The results were normalized to β-actin expression in each sample. Con means control.

deficient cells. Similar replication efficiencies were observed between pSA14 and rG66A (Fig. 3E). These results suggest that reduced propagation of rG66A mutant is related to the IFN-I response. Next, the IFN-I response induced by JEV was analyzed. We found that rG66A virus induced higher IFN-β and ISGs such as ISG15, OAS-1, and MX-1 than that by pSA14 virus in TM4 cells and A549 cells (Fig. 3F, 3G). Collectively, these results suggest that compared to the wild-type virus, the rG66A mutant induces a greater IFN-I response, which may contribute to decreased viral propagation in host cells.

JEV-NS1′ Protein Reduces Poly(I:C)-Induced Expression of IFN-I

The above results suggest that NS1′ plays a critical role in inhibiting IFN-I. To confirm this prediction, HeLa cells were transfected with plasmids encoding NS1 and NS1′, and similar amounts of NS1 and NS1′ protein were detected at 36 h post-transfection (Fig. 4A). The results showed that NS1′ rather than NS1 suppressed poly(I:C)-triggered IFN-I production and response (Fig. 4B).

To further assess the effect of NS1′ on inhibiting IFN-I during JEV replication, HeLa cells transfected with pcDNA-NS1, pcDNA-NS1′, or pcDNA3.1 were infected with rG66A or pSA14. We found that transfection of NS1′ led to increased growth of rG66A and reduced production of IFN-β and ISGs, which was similar to that of pSA14 (Fig. 4C, 4D). Taken together, these results demonstrate that NS1′ protein antagonized the production of IFN-I and ISGs, promoting the replication of JEV.

Discussion

Compared to the well-known function of NS1, few studies of NS1′ have been reported. A recent study showed that NS1′ protein has the same function as NS1 during virus replication in cells, and animal experiments clearly demonstrated that NS1′ protein enhances viral neuroinvasiveness (Young *et al.* 2013; Melian *et al.* 2010; Ye *et al.* 2012). Consistently, we showed that NS1′-deficient virus led to lower viral loads in the blood, spleen, and brain compared to its parental virus following i.p. injection. However, the two viruses showed the same virulence levels following i.c. inoculation. These findings suggest that NS1′ protein plays a crucial role in viral propagation in the peripheral tissue, which may promote JEV entry into the central nervous system.

In this study, we found that JEV NS1′ attenuated poly(I:C)-triggered IFN-I production. However, the molecular mechanism requires further analysis. Several studies clearly demonstrated the different approaches by which flaviviruses antagonize IFN-I production. For example, the NS4A protein of DENV sequesters MAVS to block IFN-I production, and WNV NS1 inhibits IFN-β responses by interacting with RIG-I and MDA5 (Dalrymple *et al.* 2015; Zhang *et al.* 2017). As observed for NS1 protein, NS1′ protein has three forms, including a monomer (intracellular protein), membrane-bound protein (mNS1′), and secreted protein (sNS1′) (Young *et al.* 2015). The region of NS1′ that performs the IFN-I function will be explored in our next study.

Interestingly, NS1′ is consistently produced by members of the JEV serogroup, such as JEV and WNV, which cause neuroinvasive disease, while other mosquito-borne flaviviruses such as DENV or YFV that produce non-neurological disease do not generate NS1′, indicating that NS1′ may play a role in neuroinvasion. Additionally, the transmission cycles of the JEV serogroup involve animals such as pigs and avian species, and studies are needed to determine whether NS1′ plays a pivotal role in virus replication/transmission in the mosquito-bird/pig cycle.

In conclusion, we demonstrated that NS1′ protein plays a crucial role in JEV pathogenesis. This is at least partially

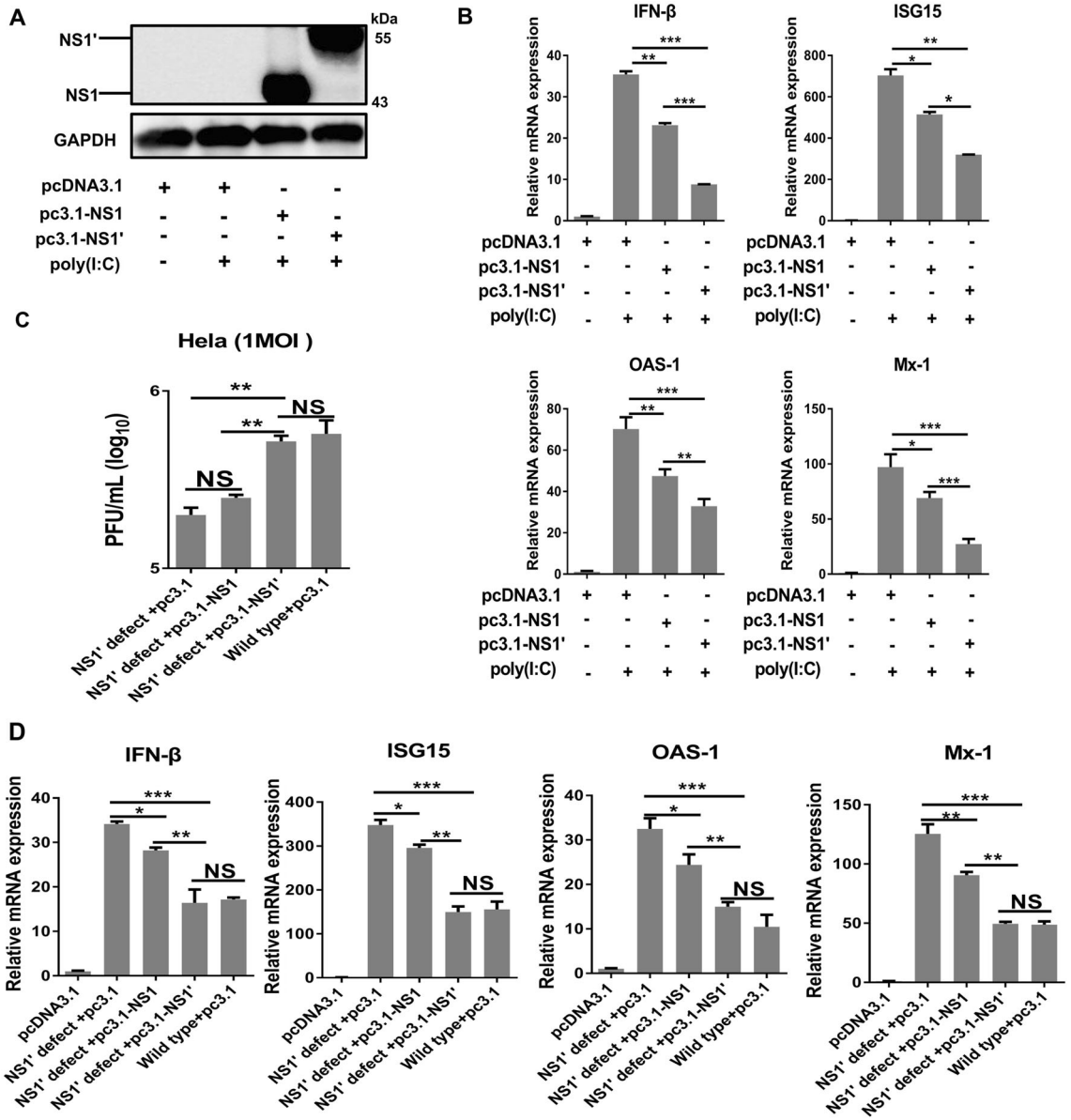

Fig. 4 JEV NS1′ reduces poly(I:C) triggered IFN-β and ISGs. **A** HeLa cells were transfected with empty vector (EV) or plasmid encoding NS1 or NS1′. Expression of JEV NS1/NS1′ protein was determined by immunoblotting at 24 h post-transfection with an anti-NS1 antibody (2B8), and GAPDH served as a reference control. **B** HeLa cells were transfected with an EV or plasmid encoding NS1 or NS1′, followed by treatment with or without poly(I:C). After 24 h of incubation, the mRNA levels of IFN-β, ISG15, OAS-1, and Mx-1 were determined by qRT-PCR. **C** Kinetics of replication of WT-pSA14 or rG66A mutant virus in HeLa cells. Cells were transfected with an empty vector or expression vector encoding NS1 or NS1′ for 12 h and then infected with WT-pSA14 or rG66A mutant virus at an MOI of 1 for 24 h. Growth kinetics from a typical experiment are shown. **D** HeLa cells were transfected with EV, or plasmid encoding NS1 or NS1′, followed by infection with WT-pSA14 or rG66A mutant virus at an MOI of 1. mRNA levels of IFN-β, ISG15, OAS-1, and Mx-1 were determined by qRT-PCR at 24 h post-infection. $*P < 0.05$, $**P < 0.01$, $***P < 0.001$. ns, no significance. All data are pooled from two or three independent experiments. The results were normalized to β-actin expression in each sample.

related to the inhibitory effect of JEV NS1′ on the IFN-I response. Our findings provide insight into JEV immune evasion mechanisms and a novel potential target for developing therapeutic methods against JEV.

Acknowledgements This work was supported by the National Key Research and Development Program of China (2016YFD0500407), National Natural Science Foundation of China (31502065 and 31572517), and Fundamental Research Funds for the Central Universities (2013PY051, 2662016Q003, and 2662015PY083).

Author Contributions JY, SBC, YFS, MC, and HCC conceived and designed the experiments. DYZ, FJ, QYL, LPZ, ZC, and ZKZ performed the experiments. DYZ analyzed the data. DYZ and JY wrote the manuscript and prepared the Figures. JY and SBC checked and

finalized the manuscript. All authors read and approved the final manuscript.

Compliance with Ethical Standards

Conflict of interest The authors declare no conflict of interests. All authors read and approved the final manuscript.

Animal and Human Rights Statement Animal experiments in this study were approved by the Scientific Ethics Committee of Huazhong Agricultural University (permit number HZAUMO-2017-016).

References

Amorim JH, Alves RP, Boscardin SB, Ferreira LC (2014) The dengue virus non-structural 1 protein: risks and benefits. Virus Res 181:53–60

Ashour J, Laurent-Rolle M, Shi PY, Garcia-Sastre A (2009) NS5 of dengue virus mediates STAT2 binding and degradation. J Virol 83:5408–5418

Best SM (2017) The many faces of the flavivirus NS5 protein in antagonism of type I interferon signaling. J Virol 91:e01970-16

Blitvich BJ, Scanlon D, Shiell BJ, Mackenzie JS, Hall RA (1999) Identification and analysis of truncated and elongated species of the flavivirus NS1 protein. Virus Res 60:67–79

Dalrymple NA, Cimica V, Mackow ER (2015) Dengue virus NS proteins inhibit RIG-I/MAVS signaling by blocking TBK1/IRF3 phosphorylation: dengue virus serotype 1 NS4A Is a unique interferon-regulating virulence determinant. mBio 6:e00553-00515

Daniels BP, Snyder AG, Olsen TM, Orozco S, Oguin TH, Tait SWG, Martinez J, Gale M, Loo YM, Oberst A (2017) RIPK3 restricts viral pathogenesis via cell death-independent neuroinflammation. Cell 169:301–313

Firth AE, Atkins JF (2009) A conserved predicted pseudoknot in the NS2A-encoding sequence of West Nile and Japanese Encephalitis flaviviruses suggests NS1′ may derive from ribosomal frameshifting. Virol J 6:14

Ginsburg AS, Meghani A, Halstead SB, Yaich M (2017) Use of the live attenuated Japanese Encephalitis vaccine SA 14-14-2 in children: a review of safety and tolerability studies. Hum Vaccin Immunother 13:2222–2231

Grant A, Ponia SS, Tripathi S, Balasubramaniam V, Miorin L, Sourisseau M, Schwarz MC, Sanchez-Seco MP, Evans MJ, Best SM, Garcia-Sastre A (2016) Zika virus targets human STAT2 to inhibit type I interferon signaling. Cell Host Microbe 19:882–890

Igarashi A, Tanaka M, Morita K, Takasu T, Ahmed A, Akram DS, Waqar MA (1994) Detection of West Nile and Japanese Encephalitis viral genome sequences in cerebrospinal fluid from acute encephalitis cases in Karachi, Pakistan. Microbiol Immunol 38:827–830

Johansen CA, van den Hurk AF, Pyke AT, Zborowski P, Phillips DA, Mackenzie JS, Ritchie SA (2001) Entomological investigations of an outbreak of Japanese Encephalitis virus in the Torres Strait, Australia, in 1998. J Med Entomol 38:581–588

Mackenzie JS (2005) Emerging zoonotic encephalitis viruses: lessons from Southeast Asia and Oceania. J Neurovirol 11:434–440

Mackenzie JS, Gubler DJ, Petersen LR (2004) Emerging flaviviruses: the spread and resurgence of Japanese Encephalitis, West Nile and Dengue viruses. Nat Med 10:S98–S109

Melian EB, Hinzman E, Nagasaki T, Firth AE, Wills NM, Nouwens AS, Blitvich BJ, Leung J, Funk A, Atkins JF, Hall R, Khromykh AA (2010) NS1′ of flaviviruses in the Japanese Encephalitis virus serogroup is a product of ribosomal frameshifting and plays a role in viral neuroinvasiveness. J Virol 84:1641–1647

Mitchell CJ, Savage HM, Smith GC, Flood SP, Castro LT, Roppul M (1993) Japanese Encephalitis on Saipan: a survey of suspected mosquito vectors. Am J Trop Med Hyg 48:585–590

Morita K, Nabeshima T, Buerano CC (2015) Japanese encephalitis. Rev Sci Tech 34:441–452

Muller DA, Young PR (2013) The flavivirus NS1 protein: molecular and structural biology, immunology, role in pathogenesis and application as a diagnostic biomarker. Antiviral Res 98:192–208

Rastogi M, Sharma N, Singh SK (2016) Flavivirus NS1: a multifaceted enigmatic viral protein. Virol J 13:131

Snell LM, Brooks DG (2015) New insights into type I interferon and the immunopathogenesis of persistent viral infections. Curr Opin Immunol 34:91–98

Sucharit S, Surathin K, Shrestha SR (1989) Vectors of Japanese Encephalitis virus (JEV): species complexes of the vectors. Southeast Asian J Trop Med Public Health 20:611–621

Teijaro JR (2016) Type I interferons in viral control and immune regulation. Curr Opin Virol 16:31–40

Turtle L, Driver C (2018) Risk assessment for Japanese Encephalitis vaccination. Hum Vaccin Immunother 14:213–217

Turtle L, Solomon T (2018) Japanese encephalitis—the prospects for new treatments. Nat Rev Neurol 14:298–313

Unni SK, Ruzek D, Chhatbar C, Mishra R, Johri MK, Singh SK (2011) Japanese encephalitis virus: from genome to infectome. Microb Infect 13:312–321

Urosevic N (2003) Is flavivirus resistance interferon type I-independent? Immunol Cell Biol 81:224–229

van den Hurk AF, Ritchie SA, Mackenzie JS (2009) Ecology and geographical expansion of Japanese Encephalitis virus. Annu Rev Entomol 54:17–35

Wang J, Li X, Gu J, Fan Y, Zhao P, Cao R, Chen P (2015) The A66G back mutation in NS2A of JEV SA14-14-2 strain contributes to production of NS1′ protein and the secreted NS1′ can be used for diagnostic biomarker for virulent virus infection. Infect Genet Evol 36:116–125

Ye Q, Li XF, Zhao H, Li SH, Deng YQ, Cao RY, Song KY, Wang HJ, Hua RH, Yu YX, Zhou X, Qin ED, Qin CF (2012) A single nucleotide mutation in NS2A of Japanese encephalitis-live vaccine virus (SA14-14-2) ablates NS1′ formation and contributes to attenuation. J Gen Virol 93:1959–1964

Young LB, Melian EB, Khromykh AA (2013) NS1′ colocalizes with NS1 and can substitute for NS1 in West Nile virus replication. J Virol 87:9384–9390

Young LB, Melian EB, Setoh YX, Young PR, Khromykh AA (2015) Last 20 aa of the West Nile virus NS1′ protein are responsible for its retention in cells and the formation of unique heat-stable dimers. J Gen Virol 96:1042–1054

Zhang HL, Ye HQ, Liu SQ, Deng CL, Li XD, Shi PY, Zhang B (2017) West Nile Virus NS1 antagonizes interferon beta production by targeting RIG-I and MDA5. J Virol 91:e02396-16